J. Mountain Res. P-ISSN: 0974-3030, E-ISSN: 2582-5011 DOI: https://doi.org/10.51220/jmr.v21-S2.20
Vol. 21(S2), (2026) 169-175

Study of Ferroelectric behaviour of H-bonded TGS, TGSe and TGFB crystals

Prabhat Chandra khanduri[1*] • Trilok Chandra Upadhyay[2]

[1]*Department of Technical Education Uttarakhand, Government Polytechnic Dehradun, Dehradun -248001, Uttarakhand, India.*
[2]*Physics Department, HNB Garhwal University (A Central University), Srinagar (Garhwal)-246174,Uttarakhand, India*

*Corresponding Author's Email Id: prabhatkhanduri@yahoo.com

Received: 24.2.2025; Revised: 30.10.2025; Accepted: 21.11.2025

Abstract : In present study we are using double time thermal Green's function method and modified pseudospin two-sublattice model by reckoning third and fourth order phonon anharmonic interactions, extra spin lattice interactions and direct spin-spin coupling to discuss ferroelectric behavior of H-bonded Triglycine sulfate (TGS), Triglycine selenate (TGSe) and Triglycine Fluoberyllate (TGFB) crystal. With the help of Dyson's equation approach and symmetric decoupling scheme theoretical formulations for shift, width, soft mode frequency, dielectric constant, loss and transition temperature have been established. Incorporating the model values of physical quantities into established theoretical formulations, temperature dependent behaviour of soft mode frequency, dielectric constant and loss have been calculated around the transition temperature. Theoretical results exhibit close conformity with the experimental results reported by others.

Keywords: TGS • TGSe • TGFB • Ferroelectric • Dielectric Constant • Soft mode frequency • Tangent loss.

Introduction

Ferroelectric materials play vital role in a range of appliances for example in form of capacitors, actuators, sensors, memory cells etc. [Kim and Kim et. al 2018, Ding and Lu et. al 2023, Mikolajick and Slesazeck et. al 2021]. These materials be included in unique group of dielectrics which demonstrates spontaneous polarization that sustained even without an external field and can be upturned by applying electric field or stress [Mikolajick 2016]. This feature of spontaneous polarization persists in a limited thermal range. Above certain temperature, called transition temperature ferroelectric material loses this feature and be converted into paraelectric[Kittel 2005]. This phase transition is associated with several properties. Emanate from the differences in phase transitions ferroelectrics are classified in two types (a) displacive type $BaTiO_3$, $KNbO_3$ etc. and (b) order-disorder type KH_2PO_4, TGS, TGFB etc.

Triglycine sulphate(TGS), Triglycine Selenate(TGSe) and Triglycine Fluoberyllate(TGFB) are ferroelectric crystal belongs to order-disorder category, undergoes phase transition at 322K, 295 K and 343K respectively[Hoshino and Mitsui et. al 1957, Jona and Shirane 1962] The lattice constants of pure TGS crystal are a=9.41Å, b=12.64Å, c=5.7Å and $\beta=110.13^0$, lattice constants of pure TGSe crystal are a=9.54Å, b=12.92Å, c=5.86Å and $\beta=110^0$ and lattice constants of pure TGFB crystal are a=9.59Å, b=12.75Å, c=5.7Å and $\beta=112^0$. The space group for TGS, TGSe and TGFB crystals are $P2_1/m$ in ferroelectric state and in paraelectric state the space group for TGS, TGSe and TGFB crystal is $P2_1$[Hoshino and Mitsui et al. 1957]. All these three crystals have similar space group symmetries [Kay and Kleinberg 1973]. These crystals contain three different glycine ions with plane mirror symmetry. This plane mirror symmetry turn out a double potential well barrier in crystal and this condition gives pseudospin character of proton between two adjacent potential wells. It is extremely important to consider bond arrangement to

explain ferroelectric behavior of crystals. Structure of TGS, TGSe and TGFB are similar apart from that SO_4^{2-} ions of TGS crystal are substituted by BeF_4^{2-} ions in TGFB and SeO_4^{2-} in TGSe crystal [Balasubramanian and Krishnan 1963, J. Przeslawski 2000]. Due to these structural changes, TGSe exhibits a specific heat peak approximately six fold greater than that observed in TGS[Ema 1983, Noheda and Lifante et. Al. 1993]. Order-disorder type phase transition is confirmed by various researchers in TGS, TGSe and TGFB crystals [Blinc and Slak 1971, Lim and Jeong 2013].

Theoretical investigations to explain ferroelectric behavior in TGS type crystals have been carried out by various methods such as Mean Field Theory [A. Mercado and J. A. Gonzalo 1973], by employing Ising type model [Gonzalo 1974], Tunneling model[Tello and Hernandez 1973], pseudo-spin lattice coupled mode model [Chaudhuri and Choudhury et al 1988, Choudhury and Chitra et. al 2004]. In current study to understand ferroelectric behaviour of TGS, TGSe and TGFB crystal we used modified pseudo-spin lattice coupled mode hereby PLCM Hamiltonian. Double time thermal dependent Green's function has been used by us in current study for obtaining formulas for shift (Δ), width (Γ), soft mode frequency $(\hat{\Omega})$, dielectric constant (ε) and loss tangent $(\tan\delta)$.

Theory

To explain ferroelectric behavior of H-bonded TGS, TGSe and TGFB crystals, the modified two sub-lattice pseudospin lattice coupled mode model Hamiltonian utilized here is given as

$$H = H_1 + H_2 + H_3 \tag{1}$$

Where

$$H_1 = -2\Omega\sum_i (S_{1i}^x + S_{2i}^x) - \sum_{ij}[J_{ij}(S_{1i}^z S_{1j}^z + S_{2i}^z S_{2j}^z) + K_{ij} S_{1i}^z S_{2j}^z] - \sum_k V_{ik}(S_{1i}^z A_k + S_{2j}^z A_k^\dagger) + \frac{1}{4}\sum_k \omega_k (A_k^\dagger A_k + B_k^\dagger B_k) \tag{2}$$

H_1 is the original Hamiltonian which is modified by adding H_2 and H_3. Here Ω shows proton tunneling frequency, S^z and S^x are representations for pseudospin variable components. J ,K, V_{ik}, A_k B_k and ω_k symbols stand for coupling among alike lattices, coupling among different lattices, spin-lattice interaction constant, position operator, momenta operator and phonon frequency correspondingly.

$$H_2 = \sum_{k_1k_2k_3} V^{(3)}(k_1,k_2,k_3) A_{k_1} A_{k_2} A_{k_3} + \sum_{k_1k_2k_3k_4} V^{(4)}(k_1,k_2,k_3,k_4) A_{k_1} A_{k_2} A_{k_3} A_{k_4} \tag{3}$$

In Hydrogen bonded crystals it is not possible to give details about numerous notable properties for instance shift appearance of central peak etc. in phase transitions without anticipating anharmonic interaction in Hamiltonian, for that reason we are considering H_2 in Hamiltonian where $V^{(3)}(k_1, k_2, k_3)$ and $V^{(4)}(k_1, k_2, k_3, k_4)$ stands for cubic and quadric-order atomic force constants correspondingly.

$$H_3 = -\sum_{ik} V_{ik} S_{1i}^x A_k - \sum_{ik} V_{ik} S_{2i}^x A_k^\dagger \tag{4}$$

H_3 stands for amendment in Ω because of non-polar phonons. This amendment takes place because of tunneling movement of protons, which amends distance along with two equilibrium positions in O—H----O bond arrangement.

Major problem in utilizing this type of Hamiltonian is to solve inhomogeneous

behavior of eigen values and eigen functions, Which are solved by Green's function method.

Here we are using double time temperature dependent Green's function:

$$G_{ij}(t-t') = \left\langle\left\langle S_i^z(t); S_j^z(t')\right\rangle\right\rangle = -i\theta(t-t')\left\langle\left[S_i^z(t), S_j^z(t')\right]\right\rangle \quad (5)$$

Angular brackets are representation for average over grand canonical ensemble and $\theta(t-t')$ stands for Heaviside's step function. We Differentiate Eq. (5) at times t and t' two times using Eq. (1), following the Fourier transforming and the application of Dyson's formalism, we arrive at,

$$G_{ij}(\omega) = \frac{\Omega\left\langle S_i^x\right\rangle\delta_{ij}}{\left[(\omega^2 - \tilde{\Omega}^2 - P(\omega)\right]} \quad (6)$$

Where

$$\tilde{\Omega}^2 = 4\Omega^2 + \frac{\left\langle\left[F,[S_{1j}^z, H]\right]\right\rangle}{2\Omega\left\langle S_i^x\right\rangle} \quad (7)$$

and

$$P(\omega) = \frac{\pi}{\Omega\left\langle S_{1i}^x\right\rangle}\left\langle\left\langle F(t); F'(t')\right\rangle\right\rangle \quad (8)$$

Within $P(\omega)$ superior order Green's function are determined through a symmetric decoupling scheme while The simpler green's functions are evaluated under Zeroth-order Shift and width are obtained as approximation. Upon Substitution of the evaluated Green's functions into $P(\omega)$ and subsequent decomposition of $P(\omega)$ into its real and imaginary components, analytical expressions for the shift $\Delta(\omega)$ and width $\Gamma(\omega)$ are obtained respectively. Green's functions finally becomes

$$G_{ij}(\omega) = \frac{\Omega\left\langle S_{1i}^x\right\rangle\delta_{ij}}{\pi\left[\omega^2 - \hat{\Omega}^2 - 2i\Omega\Gamma(\omega)\right]} \quad (9)$$

With

$$\hat{\Omega}^2 = \tilde{\Omega}^2 + 2\Omega\Delta(\omega) \quad (10)$$

$$\tilde{\Omega}^2 = (a^2 + b^2 - bc) \quad (11)$$

Where

$$a = 2J\left\langle S_1^z\right\rangle + K\left\langle S_2^z\right\rangle \quad (12)$$

$$b = 2\Omega \quad (13)$$

$$c = 2J\left\langle S_1^x\right\rangle + K\left\langle S_2^x\right\rangle \quad (14)$$

$$\Delta(\omega) = \frac{a^4}{(\omega^2-\tilde{\Omega}^2)} + \frac{b^2c^2}{(\omega^2-\tilde{\Omega}^2)} + \frac{V_{ik}{}^2N_ka^2}{(\omega^2-\tilde{\Omega}^2)} + \frac{8\Omega^2V_{ik}^2N_k}{(\omega^2-\tilde{\Omega}^2)} + \frac{a^2V_{ik}^2J_{ij}^2N_k\left\langle S_1^z\right\rangle^2}{\Omega b(\omega^2-\tilde{\Omega}^2)}$$
$$+ \frac{2V_{ik}^2J_{ij}^2N_k\left\langle S_1^x\right\rangle^2}{(\omega^2-\tilde{\Omega}^2)} + \frac{a^2V_{ik}^2K_{ij}^2N_k\left\langle S_1^z\right\rangle^2}{2b\Omega(\omega^2-\tilde{\Omega}^2)} + \frac{V_{ik}^2K_{ij}^2N_k\left\langle S_1^x\right\rangle^2}{(\omega^2-\tilde{\Omega}^2)} + \frac{a^2V_{ik}^4N_k}{\Omega b(\omega^2-\tilde{\Omega}^2)}$$
$$+ \frac{4\Omega V_{ik}{}^2\left\langle S_1^x\right\rangle\omega_k\delta_{kk'}(\omega^2-\tilde{\tilde{\omega}}_k^2)}{[(\omega^2-\tilde{\tilde{\omega}}_k^2)^2+4\omega_k^2\Gamma_k^2(\omega)]} + \frac{8\Omega aV_{ik}^2\left\langle S_1^z\right\rangle\omega_k\delta_{kk'}(\omega^2-\tilde{\tilde{\omega}}_k^2)}{b[(\omega^2-\tilde{\tilde{\omega}}_k^2)^2+4\omega_k^2\Gamma_k^2(\omega)]}$$
$$+ \frac{2V_{ik}^2J_{ij}^2\left\langle S_1^x\right\rangle\left\langle S_1^z\right\rangle^2\omega_k\delta_{kk'}(\omega^2-\tilde{\tilde{\omega}}_k^2)}{\Omega[(\omega^2-\tilde{\tilde{\omega}}_k^2)^2+4\omega_k^2\Gamma_k^2(\omega)]} + \frac{V_{ik}^2K_{ik}{}^2\left\langle S_1^x\right\rangle\left\langle S_1^z\right\rangle^2\omega_k\delta_{kk'}(\omega^2-\tilde{\tilde{\omega}}_k^2)}{\Omega[(\omega^2-\tilde{\tilde{\omega}}_k^2)^2+4\omega_k^2\Gamma_k^2(\omega)]}$$

$$\Gamma(\omega) = \frac{a^4}{2\tilde{\Omega}}\{\delta(\omega-\tilde{\Omega})-\delta(\omega+\tilde{\Omega})\} + \frac{b^2c^2}{2\tilde{\Omega}}\{\delta(\omega-\tilde{\Omega})-\delta(\omega+\tilde{\Omega})\} + \frac{V_{ik}{}^2N_ka^2}{2\tilde{\Omega}}\{\delta(\omega-\tilde{\Omega})-\delta(\omega+\tilde{\Omega})\} + \frac{8\Omega^2V_{ik}^2N_k}{2\tilde{\Omega}}\{\delta(\omega-\tilde{\Omega})-\delta(\omega+\tilde{\Omega})\}$$
$$+ \frac{a^2V_{ik}^2J_{ij}^2N_k\left\langle S_1^z\right\rangle^2}{2\Omega b\tilde{\Omega}}\{\delta(\omega-\tilde{\Omega})-\delta(\omega+\tilde{\Omega})\} + \frac{2V_{ik}^2J_{ij}^2N_k\left\langle S_1^x\right\rangle^2}{2\tilde{\Omega}}\{\delta(\omega-\tilde{\Omega})-\delta(\omega+\tilde{\Omega})\} + \frac{a^2V_{ik}^2K_{ij}^2N_k\left\langle S_1^z\right\rangle^2}{4b\Omega\tilde{\Omega}}\{\delta(\omega-\tilde{\Omega})-\delta(\omega+\tilde{\Omega})\}$$
$$+ \frac{V_{ik}^2K_{ij}^2N_k\left\langle S_1^x\right\rangle^2}{2\tilde{\Omega}}\{\delta(\omega-\tilde{\Omega})-\delta(\omega+\tilde{\Omega})\} + \frac{a^2V_{ik}^4N_k}{2b\Omega\tilde{\Omega}}\{\delta(\omega-\tilde{\Omega})-\delta(\omega+\tilde{\Omega})\} + \frac{4\Omega V_{ik}{}^2\left\langle S_1^x\right\rangle\omega_k(2\omega_k\Gamma_k(\omega))}{[(\omega^2-\tilde{\tilde{\omega}}_k^2)^2+4\omega_k^2\Gamma_k^2(\omega)]} + \frac{8\Omega aV_{ik}^2\left\langle S_1^z\right\rangle\omega_k(2\omega_k\Gamma_k(\omega))}{b[(\omega^2-\tilde{\tilde{\omega}}_k^2)^2+4\omega_k^2\Gamma_k^2(\omega)]}$$

$$+\frac{2V_{ik}^2J_{ij}^2\langle S_1^x\rangle\langle S_1^z\rangle^2\omega_k(2\omega_k\Gamma_k(\omega))}{\Omega[(\omega^2-\tilde{\tilde{\omega}}_k^2)^2+4\omega_k^2\Gamma_k^2(\omega)]}+\frac{V_{ik}^2K_{ik}^2\langle S_1^x\rangle\langle S_1^z\rangle^2\omega_k(2\omega_k\Gamma_k(\omega))}{\Omega[(\omega^2-\tilde{\tilde{\omega}}_k^2)^2+4\omega_k^2\Gamma_k^2(\omega)]}+\frac{2V_{ik}^4\langle S_1^x\rangle N_k\omega_k(2\omega_k\Gamma_k(\omega))}{\Omega[(\omega^2-\tilde{\tilde{\omega}}_k^2)^2+4\omega_k^2\Gamma_k^2(\omega)]}+\frac{2aV_{ik}^4\langle S_1^z\rangle N_k\omega_k(2\omega_k\Gamma_k(\omega))}{b\Omega[(\omega^2-\tilde{\tilde{\omega}}_k^2)^2+4\omega_k^2\Gamma_k^2(\omega)]}$$

$\tilde{\tilde{\omega}}_k$ and $\Gamma_k(\omega)$ are symbols for frequency of phonon and width of phonon respectively.

Solving Eq. (9) self consistently, soft mode frequency is achieved as

$$\hat{\Omega}^2=\frac{1}{2}(\tilde{\tilde{\omega}}_k^2+\tilde{\tilde{\Omega}}^2)\pm\frac{1}{2}\left[(\tilde{\tilde{\omega}}_k^2-\tilde{\tilde{\Omega}}^2)^2+4\left\{\begin{array}{l}4\Omega^2V_{ik}^2\langle S_1^x\rangle\omega_k+\frac{8\Omega aV_{ik}^2\langle S_1^z\rangle\omega_k}{b}+\\ \frac{2V_{ik}^2J_{ij}^2\langle S_1^x\rangle\langle S_1^z\rangle^2\omega_k+V_{ik}^2J_{ij}^2\langle S_1^x\rangle\langle S_1^z\rangle^2\omega_k}{\Omega}\\ +\frac{2V_{ik}^4\langle S_1^x\rangle N_k\omega_k}{\Omega}+\frac{2aV_{ik}^4\langle S_1^z\rangle N_k\omega_k}{b\Omega}\end{array}\right\}\right]^{1/2} \quad (15)$$

The expression for the Soft mode frequency incorporates contributions from both the modified pseudospin frequency and the renormalized phonon frequency.

By applying condition $\hat{\Omega}_- \to 0$ as $T \to T_c$ gives

$$T_c=\frac{\Omega}{2k_B\tanh^{-1}\left(\frac{4\Omega}{\tilde{J}}\right)} \quad (16)$$

Where

$$\tilde{J}=(2J-K)+\frac{2V_{ik}^2\omega_k^2}{\tilde{\tilde{\omega}}_k^2} \quad (17)$$

The relation between electrical susceptibility χ and Green's function is given as

$$\chi=-2\pi N\mu^2\left\langle\left\langle S_i^z(t);S_j^z(t')\right\rangle\right\rangle \quad (18)$$

Where N represents number of dipoles in model with dipole moment μ. The dielectric constant ε is related to χ as

$$\varepsilon=1+4\pi\chi \quad (19)$$

The expression for ε is evaluated as

$$\varepsilon=-\frac{8\pi N\mu^2\Omega\langle S_i^x\rangle(\omega^2-\hat{\Omega}_-^2)}{\left[(\omega^2-\hat{\Omega}_-^2)^2+4\Omega^2\Gamma^2(\omega)\right]} \quad (20)$$

The Green's function is represented as a combination of its real and imaginary parts and by this Eq. (20) can be written as

$$\varepsilon=\varepsilon'+i\varepsilon'' \quad (21)$$

Tangent loss can be expressed as

$$\tan\delta=\frac{\varepsilon''}{\varepsilon'} \quad (22)$$

Quality Factor can be expressed as

$$Q-Factor=\frac{1}{\tan\delta} \quad (23)$$

Results and Discussion

Model values used in calculations are given as following Table 1 and Figs 1-9.

Table 1

Ferroelectric Crystal	T_c (K)	C (k)	Ω (cm^{-1})	J (cm^{-1})	K (cm^{-1})	V_{ik} (cm^{-1})	A_k	$\mu \times 10^{18}$ Esu
TGS	322	3007	0.10	340	0	10	10.2	2.22
TGSe	295	4727	0.2	320	160	0.01	10.2	3.43
TGFB	343	3000	0.18	340	170	0.1	11.0	3.93

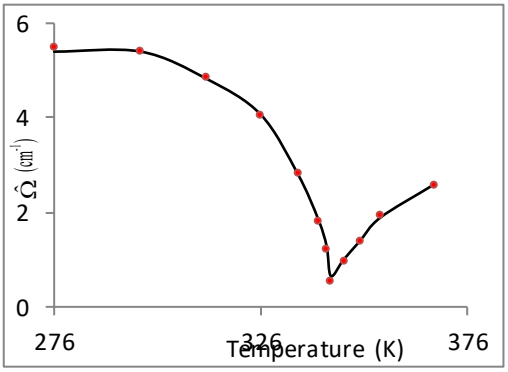

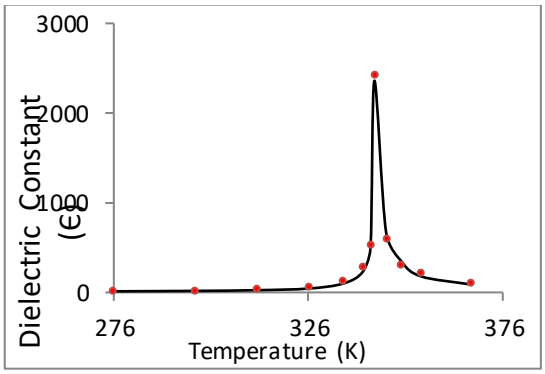

Figure (1) Thermal dependence of soft mode frequency of TGFB crystal (- present Calculation, • correlated experimental results)

Figure (2) Thermal dependence of dielectric constant of TGFB crystal (- present Calculation, • experimental results)

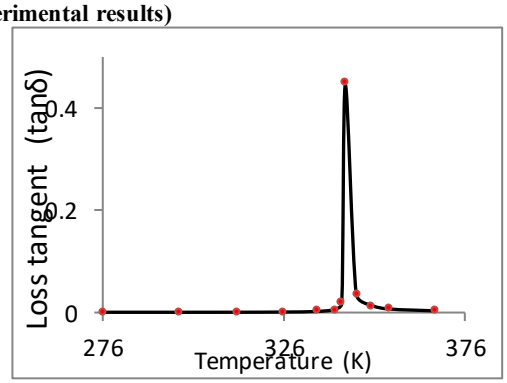

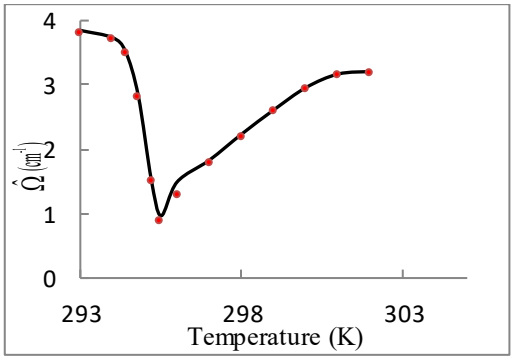

Figure (3) Thermal dependence of Loss tangent of TGFB crystal (- present Calculation, • correlated experimental results)

Figure (4) Thermal dependence of soft mode frequency of TGSe crystal (- present Calculation, • correlated experimental results)

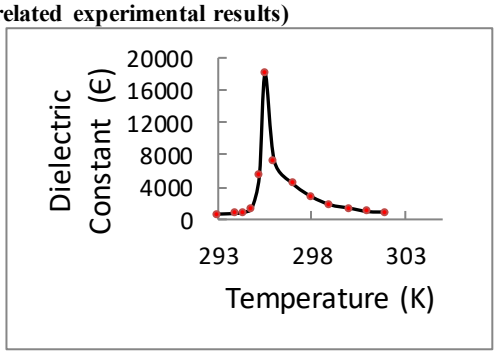

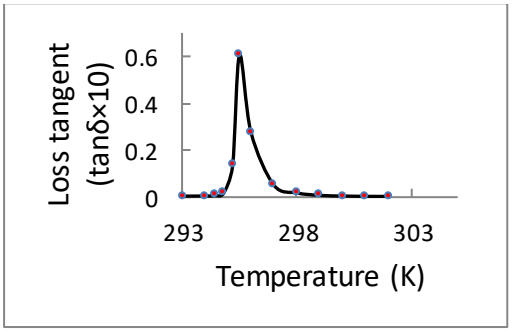

Figure (5) Thermal dependence of Dielectric constant of TGSe crystal. Crystal (- present Calculation, • experimental results)

Figure (6) Thermal dependence of tangent loss of (- present Calculation, • correlated experimental results)

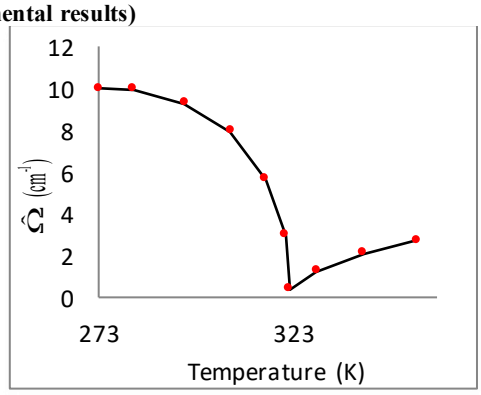

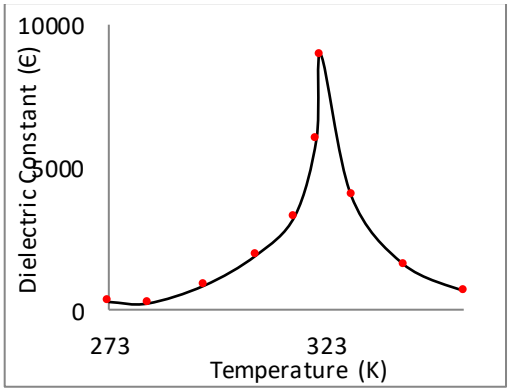

Figure (7) Thermal dependence of Soft mode frequency of TGS crystal (- present Calculation, • experimental results)

Figure (8) Thermal dependence of Dielecric constant of TGS crystal (- present Calculation, • correlated experimental results)

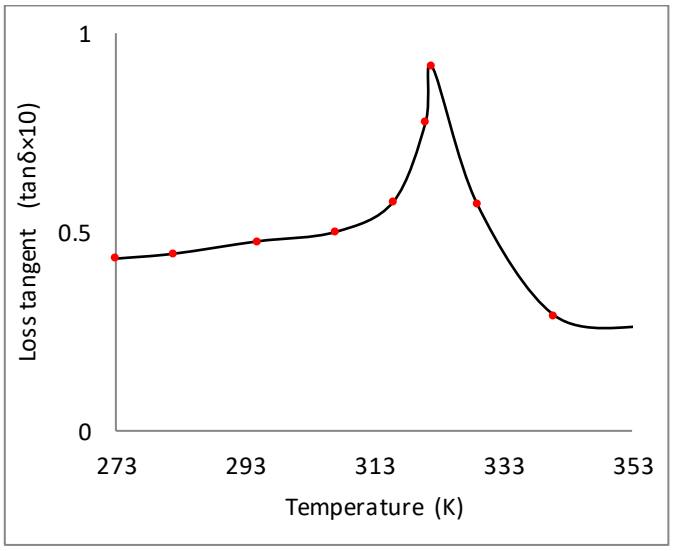

Figure (9) Thermal dependence of Loss tangent of TGS crystal (- present Calculation, • correlated experimental results)

In present theoretical work to analyze $\hat{\Omega}$, ε and $\tan\delta$ for TGS, TGSe and TGFB crystals we obtained their formulas by employing modified two sub-lattice PLCM model. Simple PLCM Hamiltonian of earlier researchers [Chaudhuri and Choudhury et al 1988] does not include third order phonon anharmonic interaction and supplementary spin-phonon interaction terms. They moreover decoupled correlations at beginning stage of calculation process, consequently few leading interactions are missing from their expressions. The shift and width terms are differences among expressions derived by us and obtained by Chaudhuri and Choudhury et al 1988 .

By putting model values in obtained formulas the variation of $\hat{\Omega}$, ε and $\tan\delta$ with respect to temperature has been examined and presented in figures 1-9 in vicinity of transition temperature. The figures clearly demonstrates that results obtained in present work are in excellent agreement with experimental values and correlated experimental values of others [Polandov and Mylov et. al 1968, Hoshino and Mitsui et al. 1957] . It is easily apparent from figure 1,4 and 7 that for all crystals TGS, TGSe and TGFB soft mode frequency gets smaller as we move towards Curie temperature (T_c) from low temperature side. At T_c value of $\hat{\Omega}$ turn into infinitesimally diminutive and raises beyond it. This behavior of $\hat{\Omega}$ demonstrates the phase transition in TGS, TGSe and TGFB crystals [Cochran 1959]. Figures 2, 3, 5, 6, 8 and 9 illustrates that both ε and $\tan\delta$ exhibit and initial increase with rising temperature, attaining maximum near T_c. Beyond T_c , both ε and $\tan\delta$ show a gradual decline with further temperature elevation.

Conclusion

In present study by utilizing Green's function (double time thermal dependent) and modified two-sublattice PLCM model we investigated ferroelectric behavior of H-bonded TGS, TGSe and TGFB crystals. Dependency of $\hat{\Omega}$, ε and $\tan\delta$ with respect to temperature is calculated and matched up to with experimental results. Theoretical results obtained by us exhibit close conformity with the experimental results reported by others, which substantiate the validity and applicability of the employed model for H-bonded TGS, TGSe and TGFB crystals. Expressions obtained here can also be making use of in explaining ferroelectric behavior of other alike crystals.

References

Blinc R, Slak J and Stepisnik J (1971). *Be quadrupole perturbed NMR study of the ferroelectric transition in deuterated triglycine fluoberyllate*, The journal of Chemical Physics, **55**,10

Chaudhuri B K, Ganguli S and Nath D (1981). *Green's-function theory of phase transitions in the hydrogen-bonded $PbHPO_4$ type ferroelectrics with pseudospin model*, Phy. Rev. B, **23**, 2308

Cochran W (1959). *Crystal stability and the theory of ferroelectricity*, Phys. Rev. Letter, **3**,412

Ding W, Lu J, Tamg X, Kou L and Liu L (2023), Ferroelectric materials and their applications in activation of small molecules, ACS Omega, **8,** 6164-6174.

Gonzalo J A (1974), Dipolar theory of ferroelectrics, Phys. Rev. B, **9**, 3149

Gordon J E and D G (1977. Boal, *Thermodynamic properties of triglycine fluoberyllate (TGFB)*, Ferroelectrics, **17**, pp. 411-414

Hoshino S, Mitsui T, Jona F and Pepinsky R (1957), Dielectric and thermal study of tri-glycine sulfate and tri-glycine fluoberyllate, Phy. Rev., **107**(5), pp. 1255.

Jona F and Shirane G 1962, Ferroelectric Crystals, Oxford : Pergamon Press.

Kim T Y, Kim S K and Kim S W,(2018). Application of ferroelectric materials for improving output power of energy harvesters, Nano convergence.

Kittel C (2005), *Introduction to Solid State Physics*, (John Wiley & Sons, New York, Eighth Edition 2005).

Lim A R and Jeong S Y (2013), *Phase transition in triglycine sulfate crystals by ^{1}H and ^{13}Cnuclear magnetic resonance in the rotating frame*, Journal of Molecular Structure, **1048**, 471-475

Mercado A and Gonzalo J A (1973). *Ferroelectric behavior of triglycine fluoberillate near T_c*, Physical Review, **7**(7) 3074

Mikolajick T (2016), *Ferroelectric nonvolatile memories*, Ref. module Mater. Sci. Mater. Eng., (Online published 2016)

Mikolajick T, Slesazeck S, Mulaosmanovic H, Park M H,Fichtner S, Lomenzo P D, Hoffmann M, Schroeder U (2021), *Next generation ferroelectric materials for semiconductor process integration and their applications*, journal of Applied Physics, **129**, 100901.

Przeslawski J (2000). *Linear birefringence derivatives for TGSe and TGFB ferroelectric crystals*, Ferroelectrics, **237**, pp. 145-152

Pulvari C F and Kuebler W (1958). *Polarization reversal in triglycine fluoberyllate and triglycine sulfate single crystals*, Journal of applied Physics, **29**, 12.

Savtinova I T Simova P D and M. Markov (1969). *Low frequency Raman scattering by ferroelectric triglycine fluoberyllate crystals*, Zhurnal Prikladnoi Spektroskopil, **10**, 3, pp. 498-501

Tello M J and Hernandez E (1973), Phenomenological Parameters in T.G.S., J Phys. Soc. Jpn., **35**, 1289

Tsedrik M S, Margolin L N and Gontarev V F (1973)., *Spontaneous polarization of triglycine selenate and triglycine fluoberyllate*, Kristall and Technik, **8**, 4, pp. 513-521

Wieder H H and C. R. Parkerson, *Some ferroelectric and dielectric properties of triglycine fluoberyllate*, J. Phys. Chem. Solids, Pergamon Press, **27**, pp.247-252 (1966).

Zubarev D N (1960). *Double-time Green's functions in statistical physics*, Sov. Phys. Uspekhi, **3**, 320